Rightward Attentional Bias in Windshield Displays:

Implication Towards External Human Machine Interfaces for Self-driving Cars

Qiang Liu, Birte Emmermann, Oscar Suen, Bryan Grant,
Jake Hercules, Erik Glaser, and Brian Lathrop
Electronic Research Laboratory (ERL)
Volkswagen Group of America
Belmont, CA. USA
extern.qiang.liu@vw.com

***Abstract* — The current paper describes research, examining the daytime lighting requirements for windshield based human machine interface (HMI) components of self-driving cars or highly autonomous vehicles (HAVs). The results of this study showed a significant rightward attentional bias in the detection of amber LEDs at low luminosity levels. The rightward bias persists at different viewing angles. However, this bias is absent for white LEDs. These results support the Saliency-Effort-Expectancy-Value (SEEV) model [12] of selective attention. These results highlight that priority should be given to the driver side for placement of critical external HMI components, especially those with lower perceptual saliency.**

Keywords—attentional bias, external HMI, lighting and illumination, safety, self-driving car

I. HMIs for Self-Driving Cars : An Issue of Saftey

Perhaps, one of the most persistent questions concerning self-driving cars, or more broadly, HAVs, involves safety — not only with respect to their internal occupants, but also those in their immediate external environment (e.g., other drivers, cyclists, pedestrians, etc.). This question is notoriously difficult to answer because it involves a multitude of factors, such as platform capability, component failure rates, and environmental complexities, just to name a few. This is precisely what led Karl and Paddock [1] to argue that exhaustive testing of HAVs in real traffic is the most logical way to assess safety. This argument itself is noncontroversial, and grounded in longstanding automotive series development practices. Rather, it is their conclusion that hundreds of millions to upwards of billions of miles must be driven first to demonstrate reliability and safety that drew consternations of researchers such as Hars [2].

While Hars' [2] issue with Karla and Paddock [1] was based on practical and methodological grounds, ours is that they [1] simply equated safety with reliability rate (or more precisely, the converse of failure rate) and relegated internal operator and occupant(s) as well as any external actors to mere passive observers. Needless to say, driving, often times, is a collective endeavor that requires active interaction with other drivers, cyclists, and pedestrians. The onus for safety is not simply the responsibility of an HAV, but also that of its internal operator/occupant(s) as well as any external actors that an HAV might potentially interact with. In other words, as with any interaction that is safety critical, effort should be made to naturally recruit as many of the internal and external participants as possible into actively contributing to the safety equation. In this respect, the efficacy of the internal and external HMIs of HAVs in increasing situation awareness (SA), conveying clear intent, and displaying functional transparency is critical to the successful execution of preventive and remedial strategies by the respective internal/external participants.

It is precisely this consideration that led the National Highway Traffic Safety Administration (NHTSA) to explicitly outline a set of minimum requirements for the internal HMIs of self-driving cars in page 24 of its Federal Automated Vehicle Policy [3]. At the same time, NHTSA recognizes that unlike internal HMIs, which have a long research history rooted in rail and aviation, external HMI research for HAVs is still very much in its infancy. Moreover, unlike rail and aviation, whose external environments are tightly controlled, the external environments of HAVs can be much more complex and congested. Thus, it highlights the pressing need for a unified and systematic approach toward the development of effective external HMIs. In this respect, we are following NHTSA's recommendation [3] that, given the rapidly evolving nature of external HAV HMI research, manufacturers should develop and apply a set of standards, guidelines, or best practices "in collaboration or consultation with relevant entities such as the Society of Automotive Engineers (SAE), International Organization for Standards (ISO), NHTSA, American National Standards (ANSI), the International Commission on illumination (CIE), and other relevant organizations.

The work reported here is a small part of this ongoing drive to establish a set of standards for the daytime lighting requirements of windshield based HMI components. This effort dovetails nicely with Endsley's [4] seminal three hierarchical phased model of SA, particularly the most basic SA level (i.e., *Level 1*), *Perception of Elements in the Environment*, "[where] the first step in achieving SA is to perceive the status, attributes, and dynamics of relevant elements in the environment (p.36)". More specifically, since Endsley's [4] model hypothesized that the development and upkeep of SA can also be affected by a number of factors (e.g., task, environmental, and individual), the current study is

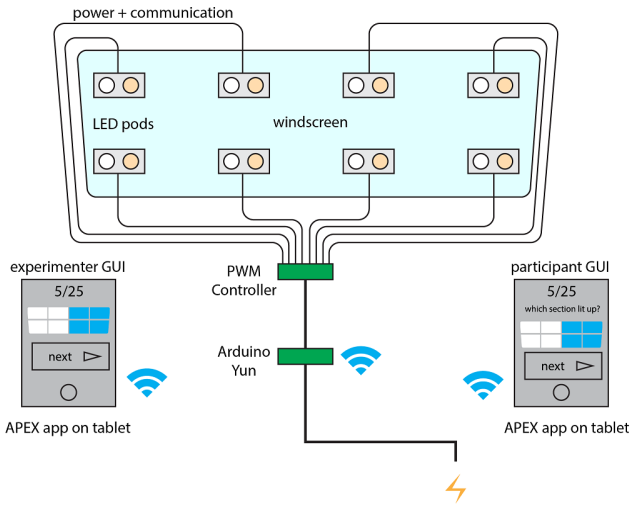

Fig. 1. Schematic of the LED display apparatus used in the current investigation of the daytime lighting requirements for windshield based HMI components.

focused squarely on identifying what are some of the key factors that may affect the allocation of visuospatial attention.

In this effort, an LED display apparatus, consisting of eight sets of LED pods, each containing two LEDs (one white and one amber), mounted on the windshield of a production 2012 Audi A7 (see Figure 1), was used to not only determine the necessary lighting values, but also identify and ascertain the effects of any potential visuospatial attention asymmetries.

II. Hypotheses of Attention Asymmetry

A. *Activation-Orientation Hypothesis*

The activation-orientation or right hemisphere (RH) dominance hypothesis [5-7] is one of the most popular explanations for the well-studied phenomenon of pseudoneglect — a mild asymmetry in visuospatial attention that favors the left side in neurologically healthy individuals [8]. Pseudoneglect have been observed in a broad range of visuospatial tasks [9], brightness discrimination, numerosity and size [10], mental imagery [11], and recently within a Lane Changing Task (LCT) [12].

Pseudoneglect, according to the activation-orientation hypothesis, occurs because visuospatial tasks involve RH activation, which produces a contralateral (i.e., leftward) attentional bias with respect to the more activated hemisphere. This account is supported by the fact that selective stimulation of the right visual field (RVF) creates a greater left hemisphere (LH) activation and thus produces a rightward shift [6]. Similarly, stimulation of the left visual field (LVF) produces a leftward shift. In this respect, because spatial attention is lateralized to the right parietal lobe, the increased RH activation in tasks with symmetric inputs naturally produces leftward biases.

This is especially important given that [12] recently reported a massive leftward bias in gaze fixations under an LCT where the driving environment was perfectly symmetric. In this respect, it is not too unreasonable to expect that different lighting requirements may be needed for different windshield regions (i.e., higher intensity levels for the rightward side) in order for an equitable performance on a perception task.

B. *The SEEV Model*

In contrast to the activation-orientation hypothesis, which is predicated on differential hemispheric activation, the SEEV model developed by [13], initially within the domain of aviation, instead focuses on the role of four core factors in the allocation of visual attention.

- ***S***aliency — the bottom up property of events/stimuli.
- ***E***ffort — the amount of movement/distance required to attend to an event.
- ***E***xpectancy — the likelihood of an event at particular locations.
- ***V***alue — the importance or relevance to the task by attending to an event.

Although [13] also accompany their theoretical model with a computational model aimed primarily at analyzing the gaze pattern distribution with respect of various "areas of interest" (AOI), our interest in and approach to the SEEV model is very similar to the selective LVF and RFV stimulation manipulation that validated the activation-orientation hypothesis. That is, whether or not selective manipulation (or the *a priori* difference) in the relative values of one or more of the four factors above will result in regional biases and performance differences.

It turns out that there may be an *a priori* difference to the value factor for different windshield regions. To illustrate this point, in a survey we administered to 205 San Francisco Bay Area residents [14], when asked what signs they would look for when crossing a street, 80% indicated that their first inclination was to look to the driver side to decipher intent (see Figure 2). This is important because in right-hand traffic countries (e.g., the US), which account for 90% of the total road distances, and traversed by 65% of the world's population

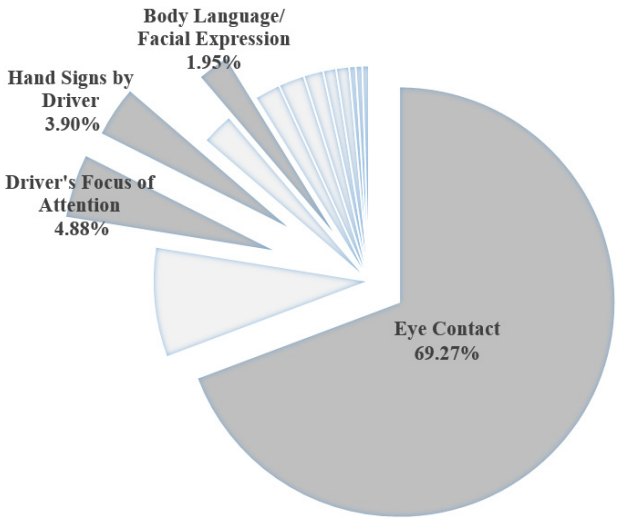

Fig. 2. 80% of the respondents surveyed reported that their first inclination is to look toward the driver to decipher intent.

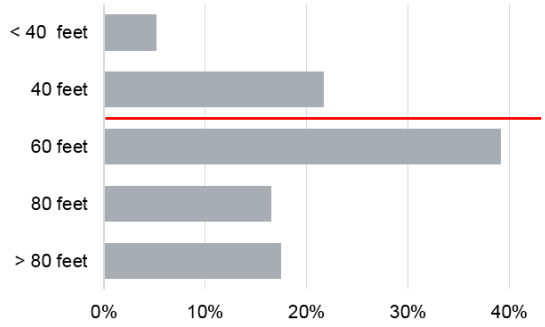

Fig. 3. 75% of the respondents we surveyed expect a car traveling at 25-40 mph to start slowing down at a distance of 60 feet or greater.

[15], the driver side from an external actor's perspective is the right-side of the windshield.

C. *Theoretical Predictions*

In this respect, it is relatively straightforward to see that with respect to the right-hand traffic environments, the activation-orientation hypothesis and the SEEV model unambiguously make opposing predictions. We should note that while stimulus saliency may play a part in the predicted asymmetry for both hypotheses, because the high value region (i.e., the driver side) in right-hand traffic countries is the right-side of the windshield from the perspective of the external actors, whether they are pedestrians, cyclists, or other drivers, the SEEV model predicts a rightward asymmetry whereas the activation-orientation hypothesis a leftward asymmetry.

III. METHOD

A. *Test Case Selection*

In the same survey we have discussed above [14], 75% of the 205 respondents also reported that they would expect a car traveling at 25-40 mph (40-65 kph) to start slowing down at a distance of 60 feet (~18 meters) or greater (see Figure 3). This result highlights that an effective external HMI would have to be perceptually salient at 60 feet (~18 meters) or greater. Given that 60-80 feet (~18-25 meters) is also the typical dimension of a two lane intersection [16], we felt that the most appropriate setting to evaluate the lighting requirements of external HMI components and test the theoretical predictions of the activation-orientation hypothesis and the SEEV model would be an environment where the most frequent pedestrian driver interactions take place. The precise dimensions of the intersection used in the current study is illustrated in Figure 4 with measurements in both English and Metric units.

B. *Viewing Angles*

The three pedestrian viewing angles for the current evaluation (see Figure 4) were based on the perspectives of a pedestrian waiting on the distal side of the street, a pedestrian in the middle of the crosswalk, and a pedestrian waiting on the proximal side of the street relative to a car waiting behind the limit line across the intersection (i.e., Angles 1, 2, and 3, respectively). These viewing angles not only offer a range of different viewpoints, but they also can be easily transposed to

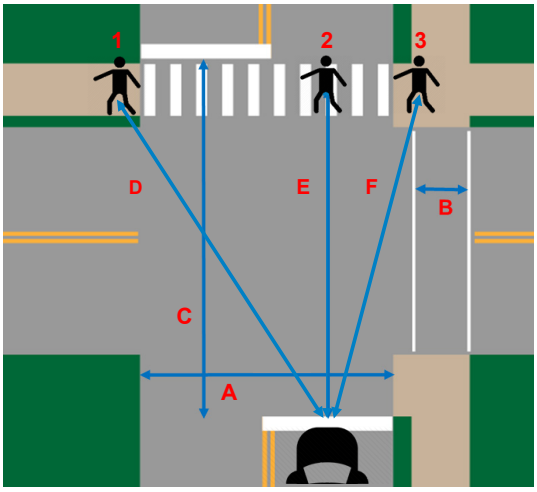

Fig. 4. The precise dimensions of the intersection used in the current evaluation are as follows: (A) Street Width = 55' (16.76m), (B) Crosswalk Width = 10' (3.05m), (C) Limit Line to Limit Line = 75' (22.86m), (D) Viewing Distance of Pedestrian 1 = 83.30' (25.39m), (E) Viewing Distance of Pedstrian 2 = 70' (21.34m), and (F) Viewing Distance of Pedestran 3 = 73.23' (22.32m). The angular offset with respect to oncoming traffic for Pedestrans 1, 2, and 3, are 34.85°, 0°, 16.89°, respectively.

the opposing crosswalk to be applicable for traffic coming from the other direction. Moreover, this reversibility allows for a straightforward extension of the current results to that of a crosswalk bisecting a street. Finally, it also affords us the opportunity of placing our mock experimental intersection in such a manner where one viewing direction will have a significant amount of glare on the vehicle's windshield, whereas the opposing direction will be negligible (see below).

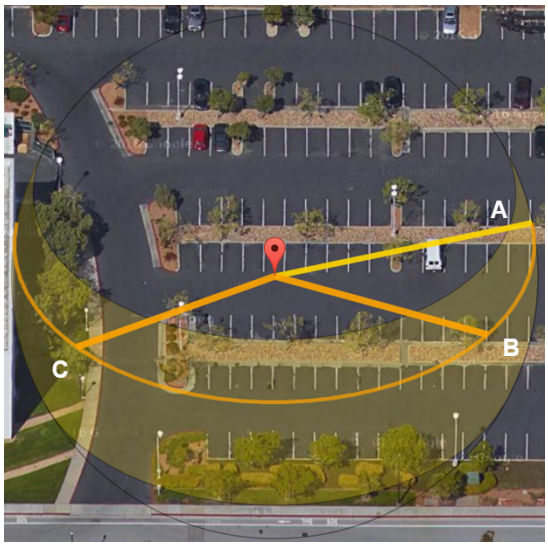

Fig. 5. The orange curve shows the trajectory of the sun within the period of August 30th to September 9th, 2016, when the current evaluation was carried out. The yellow band is the range of variation of the sun trajectories during the year. Point A denotes the position of the sun at sunrise. Point B to point C denotes the trajectory of the sun, between 9:30am to 4:30pm, during which experimental testing was carried out.

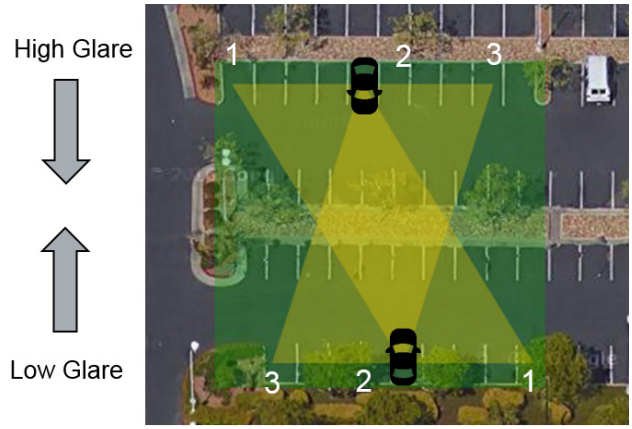

Fig. 6. Illustration of the overall experimental setup in the current evaluation. The viewing configurations for the high glare condition vis-à-vis the low glare condition are slightly offset to adapt to the dimensional limitation of the rear parking of the ERL.

C. Glare Levels, Testing Time Frame, and Experiemtal Setup

The intersection outlined in Figgure 4 is replicated in a commercial parking lot (see Figs. 5 & 6). As discussed above, because the viewing angles we selected can be easily transposed to the opposing crosswalk facing traffic coming from the other direction, it allowed us the flexibility to adjust the orientation of our mock intersection so that one viewing direction will have a very high reflective glare level, whereas the opposing viewing direction will have minimal amount glare. To this end, we used the SunCalc app developed by Vladimir Agafonkin [17] to calculate the precise trajectory of the sun during the course of the day from August 30th to September 9th, 2016, when the current evaluation was carried out (see Figure 5). Specifically, there was a minimal amount of glare when the viewing direction of the participant was facing away from the sun, and a significant amount when facing the sun (see Figure 6).

D. LED Color, Luminosity Levels, and Windshield Regions

For the current evaluation, we used the Bridgelux ES Array Series warm white LEDs (model BXRA-W0802) coupled with Ledil reflectors (model CA11183). The amber color is attained by applying a Roscolux #21 Golden Amber color effects filter on top of the reflector. To even out the any potential hot spots, Luminit Light Shaping Diffusers® are applied on top of the reflectors for both the white and amber LEDs. Moreover, to eliminate any interior reflections from showing through the windshield, a Johnson Window Films Marathon MN05 tinting film with a 5% transmission rate and a Rosco Linear Polarizing Filter with a 38% transmission rate were applied to the inside of the windshield.

For both the white and amber LEDs, four intensity levels were manually determined by the second and third authors, with level 1 being barely salient in ambient conditions under full sun, level 4 being easily visible, and levels 2 & 3 being perceptually equidistance between the two. The mean intensity levels of the white and amber LEDs at the four intensity levels measured with the tinting and polarized filter applied are listed in Table. I.

As mentioned above, the windshield of the 2012 Audi A7 used in the current evaluation was divided into eight separate regions, with each region containing one white and one amber LED placed next to each other in the geometric center of each region (see Figure 1). In total, 16 LEDs were used in the current evaluation.

TABLE. I. MEAN LUMINOSITY VALUES (LX) OF LEDS AT EACH OF THE FOUR LEVELS

	LED Intensity Level			
	1	***2***	***3***	***4***
White	67.69	254.32	420.20	562.02
Amber	156.04	218.31	354.10	482.51

[a] Note: The Lux values above reflect a 1.9% transmission rate from the LED intensity levels measured inside of the A7 given that a Johnson Window Films Marathon MN05 tinting film with a 5% transmission rate and a Rosco Linear Polarizing Filter with a 38% transmission rate were applied to the interior of the windshield.

E. Participants

A total of 18 participants (12 Males, 6 Females), ranging in age from 21 to 64 (with a mean of 40.56, SD of 13.26, and a median of 42), were recruited from the San Francisco Bay Area. All participants had normal or corrected-to-normal vision and only have right-hand traffic driving experiences.

F. Design

The design of the current experiment is a complex 2 x 3 x 2 x 4 x 8 factorial with Glare Level (high vs. low), Viewing Angles (1-3), LED Color (white vs. amber), LED Intensity (levels 1-4), and Windshield Regions (8 octants) as within subjects independent variables and detection rate as the dependent variable. The task we used was a modified Sperling's Paradigm [18]. In much of the same way as [18], participants were presented with a pseudo-randomly generated configuration of four lit LEDs (see Figure 7), and were only cued to respond whether an LED was on or off at a particular windshield region after stimulus presentation (see Figure 8). This was to ensure that participants must attend to the entire LED configuration on each trial.

The specific LED configuration presented on each trial is

Fig. 7. Example configuration of four lit LEDs presented to participants on a given trial. Note that both the hood and roof of the A7 used in the current study were covered in velvet to prevent any reflective glare on these respective regions from affecting the LED detection rates.

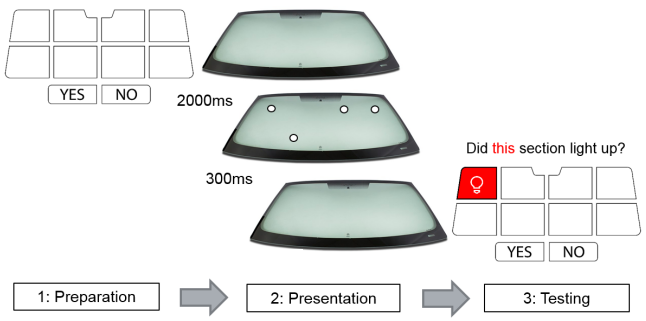

Fig. 8. On each trial, a 2 second buffer preceded stimulus presentation to give participants the time to fully fixate on the windshield. Each LED configuration was presented for 300ms. After which, participants were cued to respond to whether an LED at a specific region was lit or not. Once a response was given, the next trial was then administered.

pseudo-randomly generated because the position, status (i.e., ON or OFF), and luminosity of the critical LED was determined beforehand, whereas the position and luminosity of the remaining LEDs were randomly generated. Specifically, for each of the 16 LEDs, 24 critical trials, 12 where the LED is ON and 12 where it is OFF, were generated. For the ON trials, three separate configurations were generated at each of the four intensity levels, where the color, position, and intensity level of the three remaining lit LEDs within the seven noncritical regions were generated randomly. And for the 12 OFF trials, the color, position, and luminosity of the four lit LEDs were randomly generated within the seven noncritical regions. The position of the non-critical lit LEDs were generated without replacement in order to ensure that only one lit LED was possible for any given position. In total, three distinct sequences, each consisting of 384 pseudo-randomly generated LED configurations, were created for between subjects counterbalancing. The presentation order of the LED configurations for each of the three sequences were again pseudo-randomized to avoid the critical LED from a specific windshield regions from appearing more twice in a row. The initial viewing position, in terms of the six different viewing positions illustrated in Figure 6, was rotated clockwise across participants. For each participant, the viewing positions were switched clockwise every 32 trials.

G. Apparatus

Given that the current study took place under full sun, a Volkswagen T5, with the middle seat turned 90° facing outwards and the left sliding door wide open, was used as shade. The height of the seat was adjusted to match participants' seated eye level to their standing eye level. The T5 also doubled as seating accommodation so participants wouldn't incur fatigue from standing for a prolonged period of time.

As for the LED display apparatus, the 16 LEDs were mounted to the interior of the windshield of the A7 in eight separate LED pods, each housing a pair of LEDs (one white and one amber; see Figure 1). All of the pods were carefully aligned so they all faced outwards in parallel at the respective center of each windshield section. The pods were connected to a 16-channel pulse width modulation (PWM) driver controlled by the microcontroller. A power management system was designed and installed into the A7 experimental vehicle to sufficiently and safely operate the eight lighting pods, the PWM driver, and the microcontroller.

The experiment was controlled by two Wi-Fi connected windows tablets using a custom application written by the third and fourth authors. One of the tablets was used by the experimenter to monitor the progress of the experiment, and the other to collect the responses from participants. Communication between the tablets and the LED display apparatus was done through an Arduino Yun microcontroller over Wi-Fi. The communication between the three network-nodes were carried out using a MQ Telemetry Transport (MQTT) wireless protocol.

H. Procedure

When a participant arrived, the experimenter asked him/her to read a set of written instructions and answered any questions the participant had. The instructions indicated that a sequence of lit LED configurations would be presented on the windshield of the A7 one at a time. Participants were told that for each trial, a configuration of four lit LEDs of mixed color and intensity would be presented for 300ms. After which, they would be cued to respond whether a lit LED appeared at a specific region or not (see Figure 8). And once they respond, a two second buffer would be given for them to refocus on the windshield for the next trial.

Once participants were clear about the trial structure, they were given the participant tablet and began the testing session. They were encouraged to inform the experimenter to pause the testing whenever they felt fatigued and needed a brief break. They were also told to let the experimenter know whenever they didn't fully fixate on the windshield prior to stimulus presentation, in which case the trial would be marked and excluded from analysis.

After every 32 trials, the experimenter's tablet would pause automatically to allow to the experimenter and the driver of the T5 to move the A7 and T5 into their respective positions for the next viewing angle. The viewing positions as illustrated in Figure 6 were rotated clockwise every 32 trials. The same procedure as described above was carried out at each viewing position. Additionally, ambient light levels were measured each time the viewing orientation changed. Each experimental session took about 60 minutes to complete two full rotations of the viewing positions shown in Figure 6.

IV. Results

Given the current design complexity and difficulty in achieving a balanced factorial required for traditional ANOVAs, a multilevel mixed linear analysis was performed using the *nlme* package in R (Versions 3.31, "Bugs in Your Hair"). The model specified is a fully nested hierarchical within subjects (repeated measures) model (i.e., error term = ID / Glare Level / Viewing Angle / LED Color / LED Intensity / Windshield Region). Significant main effects of Glare Level, Viewing Angle, LED Color, LED Intensity, and Windshield

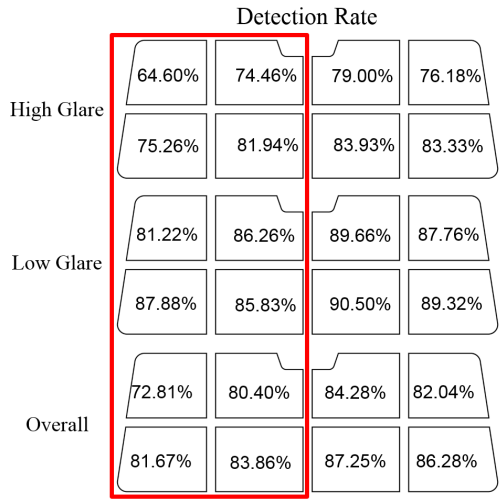

Fig. 9. Cell means of the Glare and Windshiled Position interaction displayed in terms of their respective windshield position.

Regions were observed, $F(1,17) = 17.68$, $p<0.001$, $F(2,68) = 18.58$, $p<0.001$, $F(1,102) = 14.33$, $p<0.001$, $F(3,600) = 11.85$, $p<0.001$, $F(7,1878) = 8.52$, $p<0.001$, respectively.

Significant simple interactions were also observed between LED Color and LED Intensity, LED Color and Windshield Region, LED Intensity and Windshield Region, LED Intensity and Viewing Angle, Windshield Region and Viewing Angle, and Viewing Angle and Glare Level, $F(3,600) = 4.87$, $p<0.01$, $F(7,1878) = 10.74$, $p<0.001$, $F(21,1878) = 1.60$, $p<0.05$, $F(6,600) = 5.17$, $p<0.001$, $F(14,1878) = 2.23$, $p<0.01$, $F(2,68) = 4.01$, $p<0.05$, respectively. Also, a marginally significant simple interaction was observed between Glare Level and

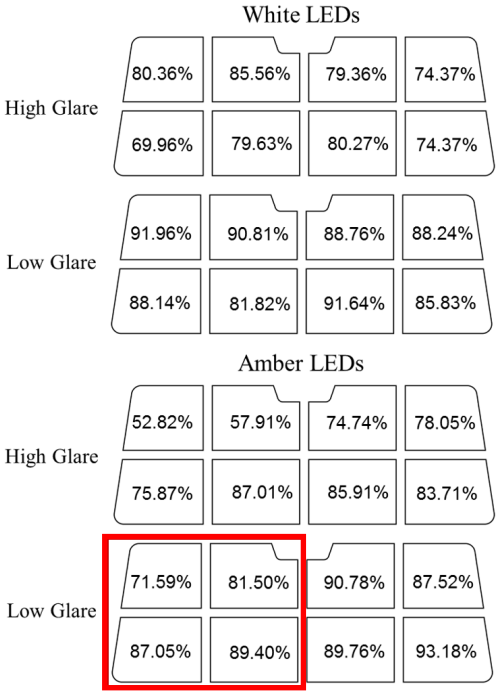

Fig.10. Cell means of the Color, Glare and Windshield Position interaction displayed in terms of their respective windshield position.

Windshield Region, $F(7,1878) = 1.99$, $p=0.0529$.

Finally, significant second order interactions were observed between LED Color, LED Intensity and Windshield Region, LED Color, Windshield Region and Glare Level, LED Color, LED Intensity and Glare Level, $F(21,1878) = 2.78$, $p<0.001$, $F(7,1754) = 2.53$, $F(3,600) = 3.11$, $p<0.05$, respectively. A marginally significant second order interaction was observed between LED Color, Windshield Region and Viewing Angle, $F(14,1878) = 1.58$, $p<0.0768$.

Though the exhaustive listing of the effects above is for completeness, what is of the most interest for the current paper is the factors behind the significant main effect of Windshield Regions and the marginally significant simple interaction between Glare Level and Windshield Region — that is, the reasons behind the differential detection rates for different regions of the windshield (see Figures 9 & 10).

A. Detection Rate Asymmetry

Figure 9 shows the mean detection rate for the different windshield regions broken down by glare levels. Although one can argue that the lower detection rate on the left (orange box) may be driven by ambient glare, this asymmetry persists even in the low glare condition. This result argues for a rightward bias that is accentuated by the presence of ambient glare.

B. Detection Rates by Color

As Figure 10 shows, the perceptual asymmetry is driven by the amber LEDs. For the white LEDs the detection rates are relatively uniform, whereas a pronounced rightward bias is observed for the amber LEDs in the low glare conditions (lower detection rates in the orange box). This asymmetry became much more pronounced under the high glare condition. This result suggests that differential allocation of attention, saliency difference between lighting components (e.g., white and amber LEDs), and ambient glare level may all exert an influence on the visibility of different windshield based HMI components.

C. Persistence at Different Viewing Angles

Though the result above is quite suggestive, one may still argue that given that the angular offsets for the three viewing positions are quite different, an apparent rightward bias may still be possible, even if the effects from different viewing angles are in the opposing direction, as long as the effect from one viewing angle is large enough. To address this explicitly, a focused analysis of the detection rates in the Low Glare condition with Viewing Angle, LED Color, and Windshield Region as factors was performed. The significant second order interactions between LED Color, Windshield Region, and Viewing Angle, $F(14, 615) = 1.99$, $p<0.05$, observed in this analysis is driven solely by the Amber LEDs. As Figure 11 shows, a rightward asymmetry, can be seen for all three viewing angles — even for viewing angles 1 and 3, where the angular offset are in the opposing direction (see Figure 4).

V. Discussion

The results of the current study are clear. There is a strong rightward bias in the detection rates of amber LEDs, but not for

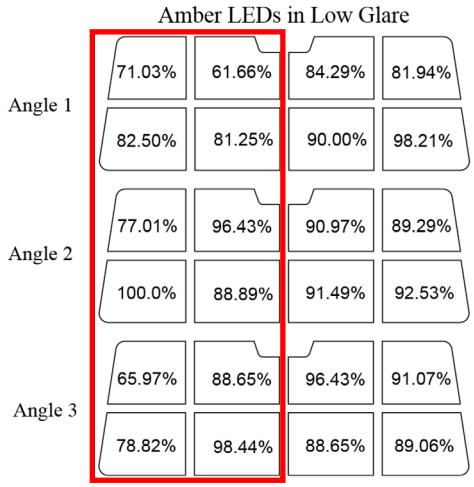

Fig.11. Detection rates of amber LEDs at different wiewing angles.

white LEDs. This effect persists across the 3 different viewing angles 3 tested. Moreover, this rightward bias is accentuated by ambient glare. The lack of a bias on white LEDs is likely due to the fact that stimulus saliency may counteract or override effects of attention allocation. Together, these results represent strong support for the SEEV model of attention allocation, but not the activation-orientation hypothesis. However, this should not be taken as a direction repudiation of the latter. Given that there is a large body of literature supporting the activation-orientation hypothesis [9, 19], it is likely the case that both hypotheses are co-viable where their respective expression may be more conducive in certain circumstances as compared to others. For example, the massive leftward gaze bias observed by [12] in an LCT may represent a situation that is much more favorable for the expression of hemispheric activation based attentional tuning, whereas the current experiment shows that for an external actor, attending to the driver side may impart high value in deciphering intent — thus, much more likely to give rise to a rightward bias.

In this respect, both [12] and the current study are important in that they showed that manufacturers must take into consideration the potential attentional asymmetries from the perspectives of the driver as well as those of the external actors. As for the current study, our results highlight that priority should be given to the driver side for placement of critical external HMI components, especially those with lower perceptual saliency.

VI. Concluding Remark and Future Work

Given that the current study is a small step towards developing a set of recommendations, guiding principles and best practices with respect to the development of effective external HMIs for self-driving cars, much more work remains for effective recruitment of all actors, both internal and external, into the safety equation.

Perhaps, the most straightforward next step is to replicate and extend the current findings to left-hand traffic environments — in which case, both the activation-orientation hypothesis and the SEEV model will predict a leftward bias. Another possibility might be to explore means to which we can alert or attract the attention of non-attentive internal/external actors in the driving environment. In short, the fast evolving nature of research into HAV external HMIs also highlight its rich research potentials.

References

[1] N. Karla, and S. M. Paddock (2016, April), “Driving to Safety: How Many Miles of Driving Would it Take to Demonstrate Autonomus Vehicle Reliability?” RAND Corporation [Web-Only]. Available: http://www.rand.org/pubs/research_reports/RR1478.html

[2] A. Hars (2016, September), “Top misconceptions of autonomous cars and self-driving vehicles, Thinking Outside the box: Inventivio Inovations Briefs, Inventivio [Web]. Available: http://www.inventivio.com/innovationbriefs/2016-09/Top-misconceptions-of-self-driving-cars.pdf

[3] NHTSA (2016, September), “Fedral Automated Vehicle Policy”, U.S. Department of Transportations, [Web]. Available: https://one.nhtsa.gov/nhtsa/av/pdf/Federal_Automated_Vehicles_Policy.pdf

[4] M. R. Endsley, “Toward a Theory of Situation Awareness in Dynamic Systems”, Human Factors, vol. 37, no. 1, pp. 32-64, 1995.

[5] M. Kinsbourne, “The cerebral basis of lateral asymmetries in attention”. Acta Psychologica, vol. 33, pp. 193–201, 1970.

[6] K. M. Heilman, and T. Van Den Abell. "Right hemisphere dominance for attention The mechanism underlying hemispheric asymmetries of inattention (neglect)." Neurology, vol. 30, no. 3, pp. 327-327, 1980.

[7] P. A. Reuter-Lorenz, M. Kinsbourne, and M. Moscovitch, “Hemispheric control of spatial attention”. Brain and Cognition, vol. 12, no. 2, pp. 240–266, 1990.

[8] D. Bowers, and K. M. Heilman, “Pseudoneglect: Effects of hemispace on a tactile line bisection task”. Neuropsychologia, vol. 18, no. 4–5, pp. 491–498, 1980.

[9] G. Jewell, and M. E. McCourt, “Pseudoneglect: A review and meta-analysis of performance factors in line bisection tasks”. Neuropsychologia, vol. 38, no. 1, pp. 93–110, 2000.

[10] M. E. R. Nicholls, and G. R. Roberts, “Can free-viewing perceptual asymmetries be explained by scanning, pre-motor or attentional biases?” Cortex, vol. 38, no. 2, pp. 113–136, 2002.

[11] P. McGeorge, N. Beschin, A. Colnaghi, M. L. Rusconi, and S. Della Sala, “A lateralized bias in mental imagery: Evidence for representational pseudoneglecy”. Neuroscience Letters, vol. 421, no. 3, pp. 259–26, 2007.

[12] S. Benedetto, M Pedrotti, R. Bremond, and T. Baccino, "Leftward attentional bias in a simulated driving task." Transportation Research Part F: Traffic Psychology and Behaviour, vol. 20, pp. 147-153, 2013.

[13] C. D., Wickens, J. Helleberg, J. Goh, X. Xu, and W. J. Horrey, “Pilot Task Management: Testing an Attentional Expected Value Model of Visual Scanning”, NASA Ames Technical Report, November, 2001.

[14] Q. Liu, and B. Emmermann, “Autonomus External HMI: Initial Large Scale Survey”, Internal Technology Report, July, 2016.

[15] "Right- and Left-hand Traffic." Wikipedia. Wikimedia Foundation, n.d. Internet: https://en.wikipedia.org/wiki/Right-_and_left-hand_traffic, Nov. 2016 [Nov. 2016].

[16] "Highway Design Manual." Caltrans Highway Design Manual. California Department of Transportation. Internet: http://www.dot.ca.gov/hq/oppd/hdm/pdf/english/HDM_Complete_16Dec2016.pdf, July. 2016 [Aug. 2016].

[17] V. Agafonkin. "SunCalc Sun Position and Sunlight Phases Calculator." SunCalc. N.p., 28. Internet: http://www.suncalc.net/#/37.5335,-122.2709,20/2016.08.30/16:28, Jan. 2011 [Nov. 2016].

[18] G. Sperling, "The information available in brief visual presentations." Psychological monographs: General and applied, vol. 74, no. 11 p. 1, 1960.

[19] C. V. Failla, D. M. Sheppard, and J. L. Bradshaw, “Age and responding-hand related changes in performance of neurologically normal subjects on the line-bisection and chimeric-faces tasks”. Brain and Cognition, vol. 52, no. 3, pp. 353–363, 2003.